Computational Assessment of Inhibitory Activity of Acridone, Xanthone and Flavone Derivatives against NS2B/NS3pro of Dengue Virus Type 2

NHV Kutumbarao[1], Chandrasekaran Ramakrishnan[2], Krishnamoorthy Balasubramanian[3] and Devadasan Velmurugan[1,*]

[1]*Centre of Advanced Study in Crystallography and Biophysics, University of Madras, Maraimalai Campus, Guindy, Chennai, India*
[2]*Department of Biotechnology, Bhupat and Jyoti Mehta School of Biosciences, Indian Institute of Technology Madras, Chennai, Tamil Nadu, India*
[3]*National Agro Foundation, Taramani, Chennai, India*

***Corresponding author:** D Velmurugan, UGC-BSR Faculty, CAS in Crystallography and Biophysics, University of Madras, Guindy Campus, Chennai, Tel: 9841075847; **E-mail:** shirai2011@gmail.com

Abstract

NS2B/NS3 protease complex plays an essential role in replication of dengue virus (DENV) in the host cell. NS3 protease is a trypsin-like serine protease and NS2B acts as a cofactor. The active site of NS3 protease contains a catalytic triad made up of His51, Asp75, and Ser135 at the N-terminal region and it is involved in cleavage of the poly-protein into single functional units. Hence, targeting NS3 protease is more important in development of more potent inhibitors to control the propagation of DENV. In this study, mode of binding of acridone and xanthones, the cyclic ketones are studied with reference to that of the experimentally proven flavones and chalcones. Docking results suggest that acridone and xanthone prefer to bind the new site (the tunnel like pocket) whereas the flavone based inhibitors and cardamonin prefer to bind the active site with the catalytic triad. Moreover, the results lead to postulate the synergistic activity of xanthone/acridone with flavone derivatives to control the DENV infection. Molecular dynamics simulation and binding free energy calculations confirm the stability of acridone and flavone which bind at the tunnel and catalytic sites, respectively.

Keywords: Dengue virus; Acridone; Xanthone; Flavone; NS2B/NS3 protease; Docking; *Flavivirus*

Introduction

Dengue virus (DENV) belongs to the *Flavivirus* genus and *Flaviviridea* family that comprises four unique serotypes *viz*., DEN-1 to DEN-4. It causes dengue hemorrhagic fever, an infectious disease in most of the tropical countries. Rapid onset of fever, joint and muscle pains, headache and appearance of rashes are the immediate symptoms upon infection [1,2]. Transmission of DENV is particularly by *Aedes aegypti*, a mosquito that commonly spread the viruses responsible for dengue fever, chikungunya, yellow fever, etc in tropical and subtropical regions. Dengue virus type 2 (Den2) is the common one of the four serotypes and its genome is a stretch of 10,732 nucleotides in the form of single-stranded positive-sense RNA. It encodes a poly protein precursor of 3,391 amino acids in length [3,4]. It is organized in the form of C-prM-E-NS1-NS2A-NS2B-NS3-NS4A-NS4B-NS5 including three structural proteins (C, prM and E) and seven non-structural proteins (NS) [5,6]. The discussions on the functional aspects of the Dengue NS2B/NS3 protease, its structural properties, drug design strategies, and resulting inhibitors are available in the literature [7-9]. In addition, the crystal structure of NS3 protease domain in complex with the 47 residue fragment of NS2B revealed the key residues involved in substrate recognition and mechanism of activation of NS3 [10] . For proteolytic cleavage of the poly-protein, the NS3 protease needs ~ 40 residue hydrophilic domain from NS2B [11]. Moreover, His51, Asp75 and Ser135, the active site residues form the catalytic triad (Figure 1) are responsible for the proteolytic activity which is the exclusive mechanism of action of serine protease family [12,13]. Lys74, Leu149 and Asn152 are located near the active site and interact with the inhibitors through hydrophobic contacts. Binding of the inhibitors induces conformational changes in the active site of NS2B/NS3pro and breaks the H-bond interaction between the Asp75 and Lys74. The NS2B/NS3 protease

complex is taken as the target for the present study for development of anti-dengue compounds [14]. Due to endemic, rate of development of inhibitors of NS2B/NS3 protease has increased. Discussion on methods of development [15,16] of some of these inhibitors is more relevant to the present work. It includes the peptido-mimetics synthesized based on the substrate peptide [17-19] or cyclo-peptides [20]. Structure-based
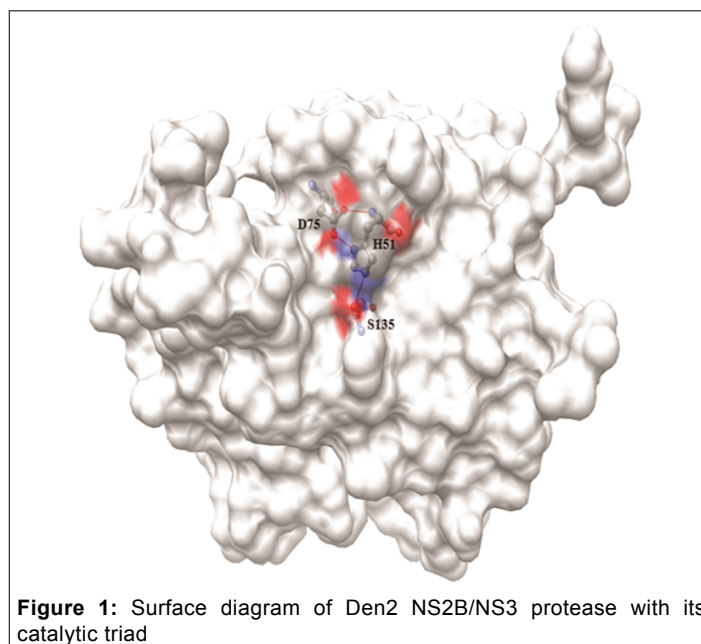

Figure 1: Surface diagram of Den2 NS2B/NS3 protease with its catalytic triad

virtual screening method was efficiently used for finding novel inhibitors [21-23]. Especially, the anthrecene based compounds ARDP0006 and ARDP0009 are structurally similar to acridone and xanthone and show considerable inhibitory activity in cell based replication assay at micro molar concentrations [22]. Similarly, library of natural products [24-26] extracted mainly from *Boesenbergia rotunda* (L.) Mansf. Kulturpfl (BRl) and a common spice of the ginger family (*Zingiberaceae*) is the source for flavone based compounds reported as inhibitors of NS2B/NS3 protease. Small molecule libraries [27] were screened to identify NS2B/NS3 specific inhibitors by in vitro high throughput screening (HTS) method and the compound BP2190 is reported as a novel and selective inhibitor [27]. Virtual screening and core hopping techniques together short listed some of the non-peptide inhibitors from ACD chemical library [28]. Nevertheless, only less number of inhibitors including peptide or small molecule inhibitors with moderate activity has been reported. Benz[d] isothiazol-3(2H)-one derivatives made by click chemistry were proven as anti-viral compounds against Den2 and West Nile virus (WNV) [29]. Derivatives of anthracene show inhibitory activity at micro molar concentrations which was proven by protease inhibitor assays and structure activity relationship (SAR) study [22]. The RC-1 peptide inhibits the NS2B-NS3pro with the IC_{50} value of 46.1 μM at 28°C, 21.4 μM at 37°C and 14.1 μM at 40°C [30]. Protegrin-1 (PG-1), a 18 a.a. peptide has been reported as a Den2 protease inhibitor by MK2 cell line based assays. It also controls the viral replication in the host and it shows the toxicity at the concentration of 12.5 μM and above [31]. Non-substrate based NS3 protease inhibitors were also reported using homology modeling, virtual screening and docking. However, there are no crystal structures available for the complex form of Den2, the NS2B/NS3pro complex with its inhibitors.

Boesenbergia rotunda L, contain a set of compounds including flavones and their corresponding chalcones was reported as good non-competitive inhibitors of Den2 protease [24]. Flavones (pinostrobin, pinocembrin and alpinetin) and their chalcones (pinostrobin chalcone, pinocembrin chalcone and cardamonin) were found to bind at the active site by the rigid and automated flexible docking methods with a good correlation between the predicted and experimental binding affinity [32]. Availability of data that support antiviral activity of some of the flavones and their chalcones are highly helpful for analysis of structurally similar compounds such as acridones and xanthones. Moreover, acridones are proven as antiviral compounds as they inhibit replication of herpes simplex virus (HSV) [33] and RNA synthesis in *Junin virus* [34]. Most importantly, activity of N-substituted acridones against haemorrhagic fever viruses like dengue were also been reported [35]. A recently published work reports the potential role of acridone and their derivatives in inhibiting the Dengue viral replication. The inhibition is found towards all the four serotypes, with increased inhibition towards DENV-2. The mode of inhibition has been studied with a host enzyme called inosine-monophospate dehydrogenase. This enzyme is believed to have an effect on viral replication by restricting the GTP synthesis [36]. The potential of acridone for anti-viral activity by viral protease inhibition and its increased efficiency by dual mode of binding is undertaken in the present study. On the other hand, xanthones are very specific group of biologically active compounds. Many of its derivatives are known to have a strong antiviral activity [37] and 20 different xanthones isolated from *Swertia mussotii* are known to inhibit viral replication in hepatitis B virus (HBV) infected cells [38]. In addition, mangosteen (*Garcinia mangostana*) fruit is one of the natural sources of many bioactive xanthones and it shows good antiviral and anticancer activities without adverse side effects. In general, both acridones and xanthones are common in terms of their inhibitory activity against the different types of Herpes Simplex Virus (HSV) [39]. Hence, the present study aims at the possibilities for inhibition of NS2B/NS3pro complex by acridone and xanthone derivatives with reference to the already reported flavone based inhibitors.

Materials and Methods

Preparation of NS2B/NS3 Protease

The crystal structure of NS3 protease in complex with the fragment of NS2B cofactor was taken from the Protein Data Bank (PDB ID: 2FOM) [10]. In the structure, a loop region is missing, which has been modelled using PRIME available in Schrödinger. The protein was prepared by assigning proper bond order and formal atomic charges. Proper ionization and tautomeric forms were ensured and optimized the H-bond network. A regular protocol of "protein preparation wizard" was used to sample the conformations of hydroxyl and thiol groups, amide group of Asn and imidazole group of His. All the amino acids (especially, Asp, Ser, Glu, Arg and His) were protonated. Before starting the docking calculation, the whole structure of the NS2B/NS3 protease was optimized and minimized with Root Mean Square Deviation (RMSD) cut off of 0.3Å in order to remove steric clashes and to calculate the conformation corresponding to (nearest) local minima.

Preparation of ligands

Flavones (pinostrobin, pinocembrin and alpinetin) and a chalcone (cardamonin) are taken as standard (known inhibitors of Den2 NS2B/NS3 protease) and their structures are depicted in figure 2. The derivatives of acridone and xanthone (Table 1) were drawn and optimized using the Chemsketch software. All these compounds were prepared for docking using "Ligprep" module available with Schrodinger Suite. The default parameters were set to generate maximum of 32 tautomers and stereoisomers at pH 7 ± 2. Steepest descent followed by conjugate gradient methods was used for energy minimisation which is available under the Impact module for convergence of structure, geometrically as well as energetically.

Compounds	Binding Site	Score	Energy (kcal/mol)
Cardamonin	Catalytic triad	-6.19	-33.87
Alpenetin	Catalytic triad	-5.34	-32.91
Pinostrobin	Catalytic triad	-5.70	-29.42
Pinocembrin	Catalytic triad	-6.57	-35.90
Acridone	Nearby the Catalytic triad	-7.83	-53.12
Xanthone	Nearby the Catalytic triad	-7.92	-50.19

Table 1: Score and energy of each compound docked with NS2B/NS3 protease
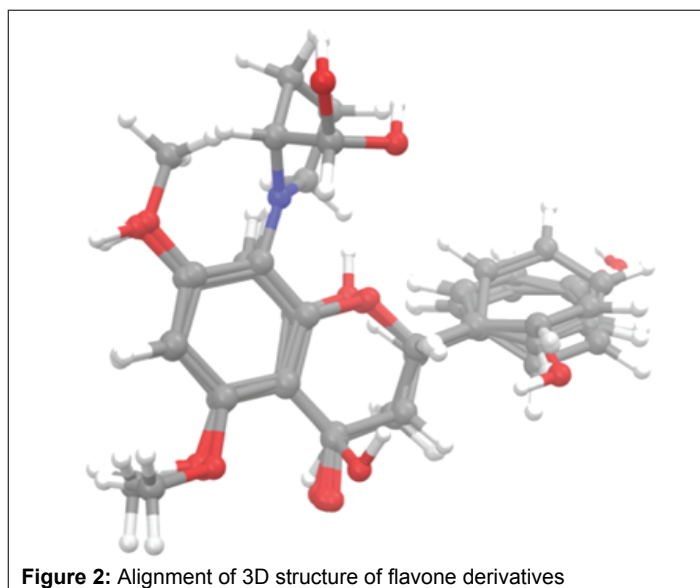

Figure 2: Alignment of 3D structure of flavone derivatives

Molecular docking

The compounds already reported based on experimental activity study were docked using induced fit docking (IFD) method [40]. It produced multiple binding poses for each ligand and ranked primarily by docking score and calculated glide energy. In this method, both the receptor and the ligand are allowed to move. Hence, the binding site can adopt the conformation that is suitable for the ligand and *vice versa*. The best pose for each standard ligand was chosen based on score, energy and the interactions. In order to find the site preference for xanthone, acridone and flavone, blind docking was performed using Glide [41] package. During the process, the grid was set to the whole protein to allow the ligands to find their binding pocket that is energetically favourable. Since the acridone and xanthone derivatives bind at the site adjacent to the catalytic site (*aka*, tunnel site), the IFD method was employed to assess the synergistic inhibition of Den2 protease by acridone and xanthone while flavones bind at catalytic site. The interactions between protein and ligand were analyzed using Ligplot [42] and Chimera [43] software packages. Optimized Potential for Liquid Simulation (OPLS-2005) [44] force field was used for all the above calculations. MD simulations were performed to confirm the stability of acridone and xanthone binding at the tunnel site while flavone binds at the catalytic site.

MD simulations

NS2B/NS3 protease in complex with each of the best scored inhibitors was simulated for 10 ns [45]. Simulation system for each protein-ligand complex was prepared using Leap module available with AMBER10 suite [46]. The established procedure was adapted to impart protonation states of the amino acids. For charge neutralization of the system, Na+ or Cl- was used. The force field parameters for acridone, xanthone and flavone derivatives were derived using antechamber program and GAFF (general amber force field) [47]. AM1-BCC charge method was used in assigning the atomic point charges [48]. The TIP3P [49] box (triangulated water molecules) with 10 Å³ box was invoked for solvation. Steepest Descent (SD) and Conjugate Gradient (CG) methods were employed to minimize the system in two phases. In the first phase, solute atoms were restrained by harmonic potential with force constant (kcal/mol-Å²) and the solvent atoms were relaxed. Then, CG method was employed to relax the whole system without restraining the solute atoms. In order to set the system to obey NPT ensemble during simulation, equilibration process was carried out in two phases. First, the temperature was equilibrated around 300 K using Berendsen temperature coupling [50], in which, 2 ps time constant was set to temperature coupling and the Maxwell distribution was used to generate random seed which was used to assign initial velocities for given temperature.

The periodic boundary condition (PBC) was implemented along with constant volume. In the second stage, isotropic positional scaling with time constant (2 ps) for pressure coupling were set to equilibrate the pressure around 1 atm. Velocity information was taken from the end of previous equilibration stage. After the equilibration, the system was interpreted in terms of the potential, kinetic and total energy as indicators to analyse the finished equilibration steps. Finally, 10 ns simulation was performed with 2 fs integration time without solute atoms being restrained. The ff03 [51,52] all atom force field was used in all the steps. Both the equilibration and MD simulations were carried out using Particle Mesh Ewald (PME) method [53] to treat the long range electrostatic interactions, SHAKE algorithm [54] to restrain all the bonds involving hydrogen atom (to control fastest vibrations), 2 fs time step and 10 Å non-bonded interaction cut-off.

Binding free energy calculation

The binding free energies (ΔG°) were calculated for complex formation between NS2B/NS3 protease and acridone or xanthone binding at tunnel site. MM-GB/SA [55-57] method and MMPBSA.py [58] module were employed for calculations involving the last 2 ns (with 5 ps frequency) of 10 ns trajectory. In MM-GB/SA method, the ff03 force field was used to calculate the MM energy (eq.2). GB method [59] was used to calculate the polar solvation energy and the molsurf [60] was used to calculate the solvent-accessible surface area (SASA). The nMode module was used by MMPBSA.py program to estimate the entropic contribution (-TΔS). The overall calculation is described in the following equations.

$$\Delta G^{\circ}_{bind,solv} = \Delta G^{\circ}_{bind,vacuum} + \Delta G^{\circ}_{solv,complex} - \left(\Delta G^{\circ}_{solv,ligand} + \Delta G^{\circ}_{solv,receptor}\right) \quad (1)$$

$$\Delta G_{bind} = \Delta H - T\Delta S \approx \Delta E_{MM} + \Delta G_{sol} - T\Delta S \quad (2)$$

$$\Delta E_{MM} = \Delta E_{internal} + \Delta E_{electrostatic} + \Delta E_{vdw} \quad (3)$$

$$\Delta G_{sol} = \Delta G_{PB/GB} + \Delta G_{SA} \quad (4)$$

Where, ΔE_{MM} is gas phase molecular mechanics energy; $-T\Delta S$ is conformational entropy; ΔG_{sol} is solvation free energy; $\Delta E_{internal}$ includes bond, angle and dihedral energies.
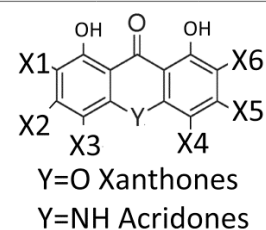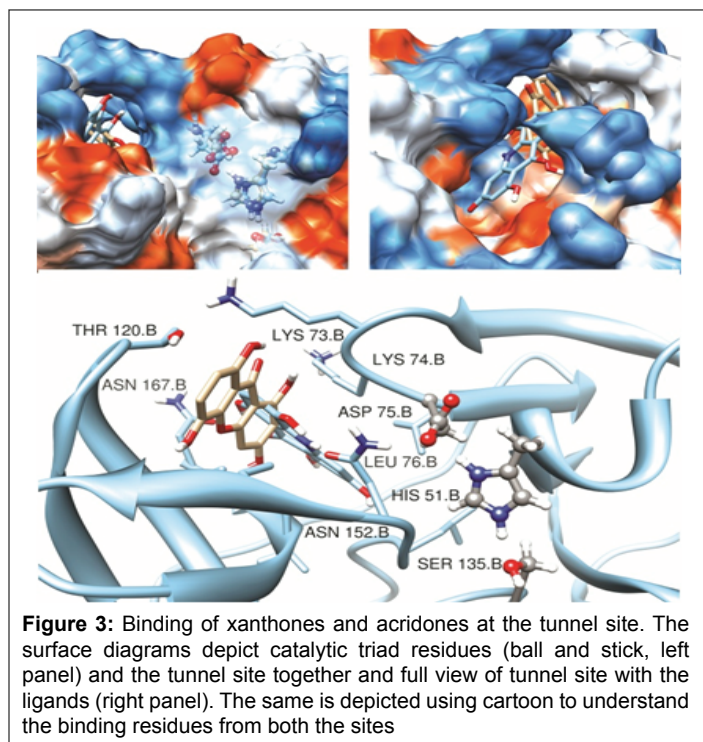
Results and Discussion

Molecular docking

As a result of IFD, 20 binding poses for each ligand were produced and the score and energy for each pose was obtained. Score of -6 ± 1 kcal/mol was observed for all the standard compounds (cardamonin, alpentin, pinocembrin and pinostrobin) (Table 1). These compounds bind well at the catalytic site and interact with all the three residues of catalytic triad and other neighboring residues through hydrogen bond and hydrophobic interactions. Score and binding energy are in comparable range as well as in the range of the values already reported in the literature [32].

Further, the nucleus structure of acridone and xanthone were subjected for Glide docking without specifying the binding site (blind-docking). Table 1 and figure 3 detail the score, energy and interactions associated with these compounds binding at the site nearby the catalytic triad (tunnel site). Both the acridone and xanthone prefer the tunnel site with score -7.8 kcal/mol which is better than that is observed for binding of standard compounds at the catalytic triad. Important characteristics of binding at the tunnel include interaction with the Lys73 and Lys74. The role of these two lysine residues is very important for binding of ligands at the catalytic triad. Binding of acridone and xanthone at the tunnel through their non-bonded interactions with Lys73 may induce conformational change at the junction of both the sites. The tunnel site is mainly composed of many hydrophobic (mainly, Lys73, Lys74 and Lue76) and few polar (mainly, Thr120 and Asn167) amino acids. This hydrophobic pocket possesses more void volume even in the presence of acridone or xanthone as shown in surface diagram in figure 3 (right panel). In order to improve the binding efficiency, different derivatives of acridone and xanthone are modelled by substituting different functional groups rich of hydrophobicity. Methyl, isopropyl and tert-butyl groups were substituted at X1 and X6 positions which are expected to improve the hydrophobicity as well as shape complementarity with the tunnel site. The details of substitutions made in both the core structures are described in table 2. The 16 derivatives for xanthone and acridone, separately, are subjected for IFD to find the favourable substitutions with good score and energy. IFD results confirm that the isopropyl group substituted at both X1 and X6 positions of both acridone and xanthone improved the binding efficiency (binding energies: -50.1 and -53.1 kcal/mole, respectively) with the interaction pattern similar to their respective core structures. Xanthone derivative has favourable score of -8 kcal/mol whereas it is -7.8 for the acridone derivative (Figure 4).

Further, docking was performed to assess the binding efficiency of each flavone derivative and the cardamonine at the catalytic triad in the presence

Figure 3: Binding of xanthones and acridones at the tunnel site. The surface diagrams depict catalytic triad residues (ball and stick, left panel) and the tunnel site together and full view of tunnel site with the ligands (right panel). The same is depicted using cartoon to understand the binding residues from both the sites

Y=O Xanthones
Y=NH Acridones

Sl. No.	X1	X2	X3	X4	X5	X6
1.	H	H	H	H	H	H
2.	Me	H	H	H	H	Me
3.	iP	H	H	H	H	iP
4.	tBu	H	H	H	H	tBu
5.	H	H	H	Me	H	H
6.	Me	H	H	Me	H	Me
7.	iP	H	H	Me	H	iP
8.	tBu	H	H	Me	H	tBu
9.	H	H	H	Me	H	H
10.	Me	H	H	Me	H	Me
11.	iP	H	H	Me	H	iP
12.	tBu	H	H	Me	H	tBu
13.	H	H	H	H	H	H
14.	Me	H	H	H	H	Me
15.	iP	H	H	H	H	iP
16.	tBu	H	H	H	H	tBu

Table 2: Derivatives made by substituting the selective functional groups in the different positions of core structure of acridone and xanthone
Functional groups: H-Hydrogen atom; Me- methyl; iP-isopropyl and tBu-tert-butyl.

of acridone and xanthone at the tunnel site. The xanthone derivative binds to the tunnel site with more number of hydrogen bond interactions than that of the acridone derivatives. The xanthone derivatives interact with Lys73, the hydrophobic amino acid present in the junction of the tunnel and the catalytic sites. In addition, these derivatives interact with Val155 and Ala166 present in the tunnel site. Apart from the hydrogen bond
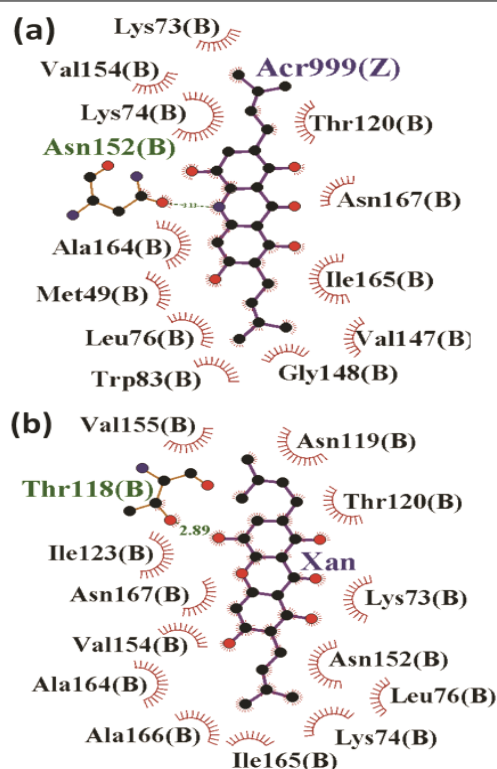

Figure 4: Binding mode of acridone (a) and xanthone (b) at the tunnel site of Den2 protease

interaction, hydrophobic contacts with the other amino acids increase the stability of the complex. On the other hand, acridone derivatives interact with Leu149 and Asn152 through hydrogen bond as well as hydrophobic interactions.

Synergism

The above results confirm that flavones and cardamonine prefer the catalytic-triad region whereas the xanthone and acridone derivatives prefer to bind at the tunnel site. Hence, the docking was performed for all the standard compounds at the catalytic triad in the presence of xanthone and acridone at tunnel site, separately. The results will be much helpful to identify the different combinations of these two groups of compounds binding at their respective sites, hence to prove the synergistic function of ligands. In the first step, the xanthone was docked at the tunnel site and screening of the standard compounds was carried out at the active site. It confirmed that the flavone binds well with the best glide energy of about -69.9 kcal/mol . Similarly, the acridone derivative was fixed at the tunnel region and the screening was carried out at the triad where acridone derivative shows good binding energy (-53.1 kcal/mol) (Figure 5a). In the presence of acridone at tunnel site, binding energy for flavone to bind the active site (catalytic triad) is -40.7 kcal/mol (Figure 5b). This is highly unfavourable when compared to its binding in the presence of xanthone (in the place of acridone) (Figure 5c). The binding free energy calculated (entropy term included) based on the MD simulation trajectory substantiates well the above docking results (Figure 6). Acridone binds very strongly (-24 kcal/mol) compared to the xanthone (-6 kcal/mol). Binding of second acridone (at catalytic triad) is not favourable (< -3kcal/mol) whereas flavone binds well (-4 kcal/mol). Similarly, flavone shows more favourable binding (-7.5 kcal/mol) in the presence of xanthone at the tunnel site. During synergistic inhibition with flavone, acridone binds tunnel site with more affinity (-12.5 kcal/mol) compared to the xanthone (<-3 kcal/mol). Together, acridone and flavone show favourable binding
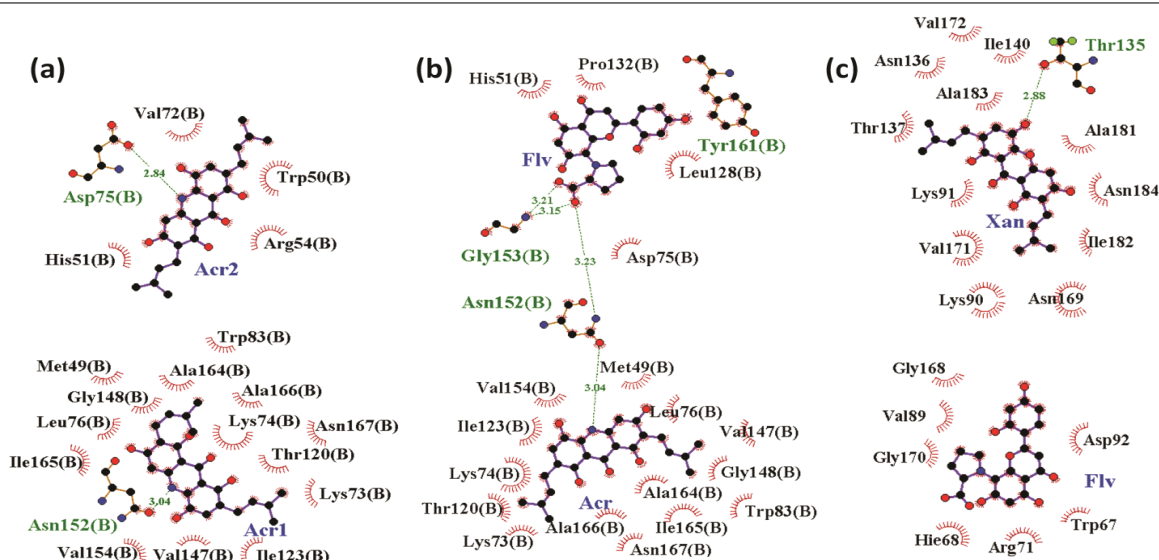
Figure 5: Synergistic binding mode of acridone and xanthone at tunnel site while flavone/acridone binds in catalytic site
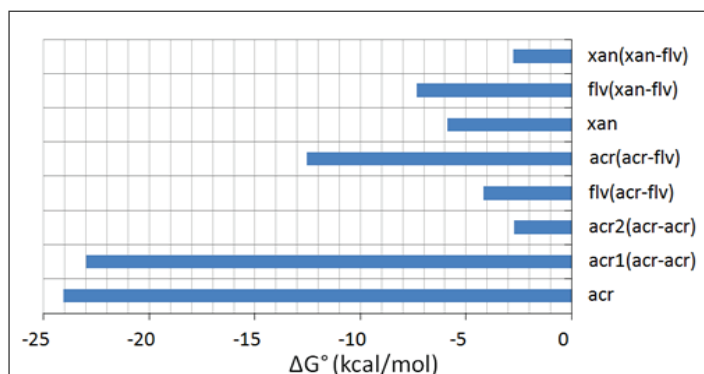

Figure 6: Binding free energy (ΔG°=ΔH-TΔS) calculated for binding of acridone and xanthone at the tunnel site in the presence of flavone at catalytic site. In acr#(acr-acr), possibility for acridone to bind both the sites, where, acr1 denotes binding of acridone at the catalytic site and acr2 denotes binding of acridone at the tunnel site

with their preferred sites suggesting that these two compounds will have synergistic inhibitory activity against the proteolytic activity of NS2B/NS3pro.

Conclusion

Flexible docking studies confirm that the flavone and chalcone based inhibitors of DENV NS2B/NS3pro prefer to bind the active site with the catalytic triad. The acridone and xanthone based compounds are known to have antiviral activity and they tend to bind at the new site nearby the catalytic triad, called tunnel site. This provides a new insight in designing inhibitors for DENV based on the structure of NS2B/NS3 protease. Also, it provides a base to propose that a synergism can exist in the inhibitory activity of these two site specific inhibitors. Flexible docking , MD simulation and binding free energy calculations confirm that acridone and flavone based compounds will synergistically inhibit DENV NS2B/NS3 protease complex and this new finding provides the base for further extension with biochemical and structural studies to confirm the same. Binding studies for the dual inhibition sites have not been reported so far. As a continuation of the present work, binding studies with anti-viral compounds from natural resources are being undertaken with NS2B/NS3 protease.

References

1. Whitehorn J, Farrar J (2010) Dengue. Br Med Bull 95: 161-173.
2. Chen LH, Wilson ME (2010) Dengue and chikungunya infections in travelers. Curr Opin Infect Dis 23: 438-444.
3. Zhang L, Mohan PM, Padmanabhan R (1992) Processing and localization of Dengue virus type 2 polyprotein precursor NS3-NS4A-NS4B-NS5. J Virol 66: 7549-7554.
4. Irie K, Mohan PM, Sasaguri Y, Putnak R, Padmanabhan R (1989) Sequence analysis of cloned dengue virus type 2 genome (New Guinea-C strain). Gene 75: 197-211.
5. Cahour A, Falgout B, Lai CJ (1992) Cleavage of the dengue virus polyprotein at the NS3/NS4A and NS4B/NS5 junctions is mediated by viral protease NS2B-NS3, whereas NS4A/NS4B may be processed by a cellular protease. J Virol 66: 1535-1542.
6. Preugschat F, Yao CW, Strauss JH (1990) In vitro processing of dengue virus type 2 nonstructural proteins NS2A, NS2B, and NS3. J Virol 64: 4364-4374.
7. Steuber H, Hilgenfeld R (2010) Recent advances in targeting viral proteases for the discovery of novel antivirals. Curr Top Med Chem 10: 323-345.
8. Tong L (2002) Viral proteases. Chem Rev 102: 4609-4626.
9. Steuer C, Gege C, Fischl W, Heinonen KH, Bartenschlager R, et al. (2011) Synthesis and biological evaluation of α-ketoamides as inhibitors of the Dengue virus protease with antiviral activity in cell-culture. Bioorg Med Chem 19: 4067-4074.
10. Erbel P, Schiering N, D'Arcy A, Renatus M, Kroemer M, et al. (2006) Structural basis for the activation of flaviviral NS3 proteases from dengue and West Nile virus. Nat Struct Mol Biol 13: 372-373.
11. Yusof R, Clum S, Wetzel M, Murthy HM, Padmanabhan R (2000) Purified NS2B/NS3 serine protease of dengue virus type 2 exhibits cofactor NS2B dependence for cleavage of substrates with dibasic amino acids in vitro. J Biol Chem 275: 9963-9969.

12. Chambers TJ, Nestorowicz A, Amberg SM, Rice CM (1993) Mutagenesis of the yellow fever virus NS2B protein: effects on proteolytic processing, NS2B-NS3 complex formation, and viral replication. J Virol 67: 6797-6807.

13. Bazan JF, Fletterick RJ (1989) Detection of a trypsin-like serine protease domain in flaviviruses and pestiviruses. Virology 171: 637-639.

14. Falgout B, Pethel M, Zhang YM, Lai CJ (1991) Both nonstructural proteins NS2B and NS3 are required for the proteolytic processing of dengue virus nonstructural proteins. J Virol 65: 2467-2475.

15. Lescar J, Luo D, Xu T, Sampath A, Lim SP, et al. (2008) Towards the design of antiviral inhibitors against flaviviruses: the case for the multifunctional NS3 protein from Dengue virus as a target. Antiviral Res 80: 94-101.

16. Noble CG, Chen YL, Dong H, Gu F, Lim SP, et al. (2010) Strategies for development of Dengue virus inhibitors. Antiviral Res 85: 450-462.

17. Yin Z, Patel SJ, Wang WL, Chan WL, Ranga Rao KR, et al. (2006) Peptide inhibitors of dengue virus NS3 protease. Part 2: SAR study of tetrapeptide aldehyde inhibitors. Bioorg Med Chem Lett 16: 40-43.

18. Yin Z, Patel SJ, Wang WL, Wang G, Chan WL, et al. (2006) Peptide inhibitors of Dengue virus NS3 protease. Part 1: Warhead. Bioorg Med Chem Lett 16: 36-39.

19. Chanprapaph S, Saparpakorn P, Sangma C, Niyomrattanakit P, Hannongbua S, et al. (2005) Competitive inhibition of the dengue virus NS3 serine protease by synthetic peptides representing polyprotein cleavage sites. Biochem Biophys Res Commun 330: 1237-1246.

20. Gao Y, Cui T, Lam Y (2010) Synthesis and disulfide bond connectivity-activity studies of a kalata B1-inspired cyclopeptide against dengue NS2B-NS3 protease. Bioorg Med Chem 18: 1331-1336.

21. Tomlinson SM, Malmstrom RD, Russo A, Mueller N, Pang YP, et al. (2009) Structure-based discovery of dengue virus protease inhibitors. Antiviral Res 82: 110-114.

22. Tomlinson SM, Watowich SJ (2011) Anthracene-based inhibitors of dengue virus NS2B-NS3 protease. Antiviral Res 89: 127-135.

23. Knehans T, Schuller A, Doan DN, Nacro K, Hill J, et al. (2011) Structure-guided fragment-based in silico drug design of dengue protease inhibitors. J Comput Aided Mol Des 25: 263-274.

24. Kiat TS, Pippen R, Yusof R, Ibrahim H, Khalid N, et al. (2006) Inhibitory activity of cyclohexenyl chalcone derivatives and flavonoids of fingerroot, Boesenbergia rotunda (L.), towards dengue-2 virus NS3 protease. Bioorg Med Chem Lett 16: 3337-3340.

25. Hidari KI, Takahashi N, Arihara M, Nagaoka M, Morita K, et al. (2008) Structure and anti-dengue virus activity of sulfated polysaccharide from a marine alga. Biochem Biophys Res Commun 376: 91-95.

26. Frimayanti N, Chee CF, Zain SM, Rahman NA (2011) Design of new competitive dengue ns2b/ns3 protease inhibitors-a computational approach. Int J Mol Sci 12: 1089-1100.

27. Yang CC, Hsieh YC, Lee SJ, Wu SH, Liao CL, et al. (2011) Novel dengue virus-specific NS2B/NS3 protease inhibitor, BP2109, discovered by a high-throughput screening assay. Antimicrob Agents Chemother 55: 229-238.

28. Deng J, Li N, Liu H, Zuo Z, Liew OW, et al. (2012) Discovery of novel small molecule inhibitors of dengue viral NS2B-NS3 protease using virtual screening and scaffold hopping. J Med Chem 55: 6278-6293.

29. Tiew KC, Dou D, Teramoto T, Lai H, Alliston KR, et al. (2012) Inhibition of Dengue virus and West Nile virus proteases by click chemistry-derived benz[d]isothiazol-3(2H)-one derivatives. Bioorg Med Chem 20: 1213-1221.

30. Rothan HA, Han HC, Ramasamy TS, Othman S, Rahman NA, et al. (2012) Inhibition of dengue NS2B-NS3 protease and viral replication in Vero cells by recombinant retrocyclin-1. BMC Infect Dis 12: 314.

31. Rothan HA, Abdulrahman AY, Sasikumer PG, Othman S, Rahman NA, et al. (2012) Protegrin-1 inhibits dengue NS2B-NS3 serine protease and viral replication in MK2 cells. J Biomed Biotechnol 2012: 251482.

32. Othman R, Kiat TS, Khalid N, Yusof R, Newhouse EI, et al. (2008) Docking of noncompetitive inhibitors into dengue virus type 2 protease: understanding the interactions with allosteric binding sites. J Chem Inf Model 48: 1582-1591.

33. Yamamoto N, Furukawa H, Ito Y, Yoshida S, Maeno K, et al. (1989) Anti-herpesvirus activity of citrusinine-I, a new acridone alkaloid, and related compounds. Antiviral Res 12: 21-36.

34. Sepulveda CS, Garcia CC, Fascio ML, D'Accorso NB, Docampo Palacios ML, et al. (2012) Inhibition of Junin virus RNA synthesis by an antiviral acridone derivative. Antiviral Res 93: 16-22.

35. Sepulveda CS, Fascio ML, Mazzucco MB, Palacios ML, Pellon RF, et al. (2008) Synthesis and evaluation of N-substituted acridones as antiviral agents against haemorrhagic fever viruses. Antivir Chem Chemother 19: 41-47.

36. Mazzucco MB, Talarico LB, Vatansever S, Carro AC, Fascio ML, et al. (2015) Antiviral activity of an N-allyl acridone against dengue virus. J Biomed Sci 22: 29.

37. Shan T, Ma Q, Guo K, Liu J, Li W, et al. (2011) Xanthones from mangosteen extracts as natural chemopreventive agents: potential anticancer drugs. Curr Mol Med 11: 666-677.

38. Cao TW, Geng CA, Ma YB, He K, Wang HL, et al. (2013) Xanthones with anti-hepatitis B virus activity from Swertia mussotii. Planta Med 79: 697-700.

39. Goodell JR, Madhok AA, Hiasa H, Ferguson DM (2006) Synthesis and evaluation of acridine- and acridone-based anti-herpes agents with topoisomerase activity. Bioorg Med Chem 14: 5467-5480.

40. Sherman W, Day T, Jacobson MP, Friesner RA, Farid R (2006) Novel procedure for modeling ligand/receptor induced fit effects. J Med Chem 49: 534-553.

41. Friesner RA, Banks JL, Murphy RB, Halgren TA, Klicic JJ, et al. (2004) Glide: A New Approach for Rapid, Accurate Docking and Scoring. 1. Method and Assessment of Docking Accuracy. Journal J Med Chem 47: 1739-1749.

42. Wallace AC, Laskowski RA, Thornton JM (1995) LIGPLOT: a program to generate schematic diagrams of protein-ligand interactions. Protein Eng 8: 127-134.

43. Pettersen EF, Goddard TD, Huang CC, Couch GS, Greenblatt DM, et al. (2004) UCSF Chimera- A visualization system for exploratory research and analysis. J Comput Chem 25: 1605-1612.

44. Jorgensen WL (1981) Quantum and statistical mechanical studies of liquids. 10. Transferable intermolecular potential functions for water, alcohols, and ethers. Application to liquid water. J Am Chem Soc 103: 335-340.

45. Ramakrishnan C, Joshi V, Joseph JM, Vishwanath BS, Velmurugan D (2014) Identification of Novel Inhibitors of Daboia russelli Phospholipase A2 Using the Combined Pharmacophore Modeling Approach. Chem Biol Drug Des 84: 379-392.

46. Pearlman DA, Case DA, Caldwell JW, Ross WS, Cheatham Iii TE, et al. (1995) AMBER, a package of computer programs for applying molecular mechanics, normal mode analysis, molecular dynamics and free energy calculations to simulate the structural and energetic properties of molecules. Comput Phys Commun 91: 1-41.

47. Wang J, Wolf RM, Caldwell JW, Kollman PA, Case DA (2004) Development and testing of a general amber force field. J Comput Chem 25: 1157-1174.

48. Jakalian A, Bush BL, Jack DB, Bayly CI (2000) Fast, efficient generation of high-quality atomic charges. AM1-BCC model: I. Method. J Comput Chem 21: 132-146.

49. Jorgensen WL, Chandrasekhar J, Madura JD, Impey RW, Klein ML (1983) Comparison of simple potential functions for simulating liquid water. J Chem Phys 79: 926-935.

50. Berendsen HJC, Postma JPM, van Gunsteren WF, DiNola A, Haak JR (1984) Molecular dynamics with coupling to an external bath. J Chem Phys 81: 3684-3690.

51. Ponder JW, Case DA (2003) Force fields for protein simulations. Adv Protein Chem 66: 27-85.

52. Duan Y, Wu C, Chowdhury S, Lee MC, Xiong G, et al. (2003) A point-charge force field for molecular mechanics simulations of proteins based on condensed-phase quantum mechanical calculations. J Comput Chem 24: 1999-2012.

53. Darden T, York D, Pedersen L (1993) Particle mesh Ewald: An *N.log(N)* method for Ewald sums in large systems. J Chem Phys 98: 10089-10092.

54. Ryckaert J-P, Ciccotti G, Berendsen HJC (1977) Numerical integration of the cartesian equations of motion of a system with constraints: molecular dynamics of n-alkanes. J Comput Phys 23: 327-341.

55. Wang J, Hou T, Xu X (2006) Recent Advances in Free Energy Calculations with a Combination of Molecular Mechanics and Continuum Models. Current Computer - Aided Drug Design 2: 287-306.

56. Wang W, Donini O, Reyes CM, Kollman PA (2001) Biomolecular simulations: recent developments in force fields, simulations of enzyme catalysis, protein-ligand, protein-protein, and protein-nucleic acid noncovalent interactions. Annu Rev Biophys Biomol Struct 30: 211-243.

57. Kollman PA, Massova I, Reyes C, Kuhn B, Huo S, et al. (2000) Calculating Structures and Free Energies of Complex Molecules: Combining Molecular Mechanics and Continuum Models. Acc Chem Res 33: 889-897.

58. Miller BR, McGee TD, Swails JM, Homeyer N, Gohlke H, et al. (2012) MMPBSA.py: An Efficient Program for End-State Free Energy Calculations. J Chem Theory Comput 8: 3314-3321.

59. Onufriev A, Bashford D, Case DA (2004) Exploring protein native states and large-scale conformational changes with a modified generalized born model. Proteins 55: 383-394.

60. Connolly M (1983) Analytical molecular surface calculation. J Appl Cryst 16: 548-558.